Integrated Optical Fiber-tip Cantilevers

Christopher Holmes, Alexander Jantzen, Alan C Gray, Lewis G Carpenter, Paul C Gow, Stephen G Lynch, James C Gates and Peter G R Smith

***Abstract*— A microcantilever at the end face of an integrated optical fiber is reported, fabrication is uniquely achieved using a precision dicing saw. The methodology is a single-step rapid process, capable of achieving trenches with high aspect ratio (>10:1). The platform on which fabrication is made is a monolithic, integrated optical fiber. This integrally fuses optical fiber to a planar substrate using flame hydrolysis deposition (FHD) and high temperature consolidation (>1000°C). This paper is the first report of a fiber-tip cantilever using the technique and this integrated platform. As an approach to quantify the optical response of such a multicavity arrangement, a method using Mason's rule is presented. This is used to infer the spectral responses of individual cavities formed and through physical actuation, an estimation of the cantilever's spring constant is made.**

***Index Terms*—Integrated Optics, Optical Fiber Devices, Optical Fibers, Optical Interferometry, Optical Sensors**

I. Introduction

OPTICAL alternatives to Microelectromechanical Systems (MEMS) are becoming of increasing interest to science and technology due to their immunity to electromagnetic interference, inherent safety in flammable environments and compatibility with optical-fiber. Recent developments in forming cantilevers at the tip of optical fibers have opened-up exciting new opportunities for miniaturized optical sensors [1]–[3]. In particular measurements of fluidic flow [4], bio-mechanical characterization [5], [6], Atomic Force Microscopy (AFM) imaging [7], and chemical sensing [8] have all recently demonstrated using this format. Typically these systems use Fabry-Pérot (FP) interferometry for monitoring, largely due to the inherent cavity formed between the fiber and cantilever. The spectral response from such cavities generally has a low-finesse due to the weak Fresnel reflections from the silica-air interfaces. However, in some fabrication methodologies finesse can be enhanced through use of additional coatings. The physical fabrication approaches reported thus far have included picosecond-laser machining [4], focused ion beam [9], wire-cut micromachining [6] and photolithography [10].

This work was supported by Research Council UK, Engineering and Physical Sciences Research Council, UK Quantum Technology Hub, Sensors and Metrology, EP/M013294/1. The authors are all affiliated to the Optoelectronics Research Centre, University of Southampton, Southampton, SO17 1BJ, UK. Dr Christopher Holmes (e-mail: christopher.holmes@southampton.ac.uk).

This work reports cantilever fabrication solely through the use of physical micromachining [11]. The technique has the advantages of removing large amounts of material (mm^3) quickly (minutes) whilst still maintaining a vertical form factor. The platform chosen on which to demonstrate this technique is a novel Integrated Optical Fiber (IOF) [12], [13], illustrated in Figure 1. IOF uses Flame Hydrolysis Deposition (FHD) to robustly form a miscible alloy between the optical fiber and the planar substrate. IOF offers superior mechanical strength and has advantages associated with integration including thermal homogeneity and the ability to fabricate multiple components upon a single compact chip.

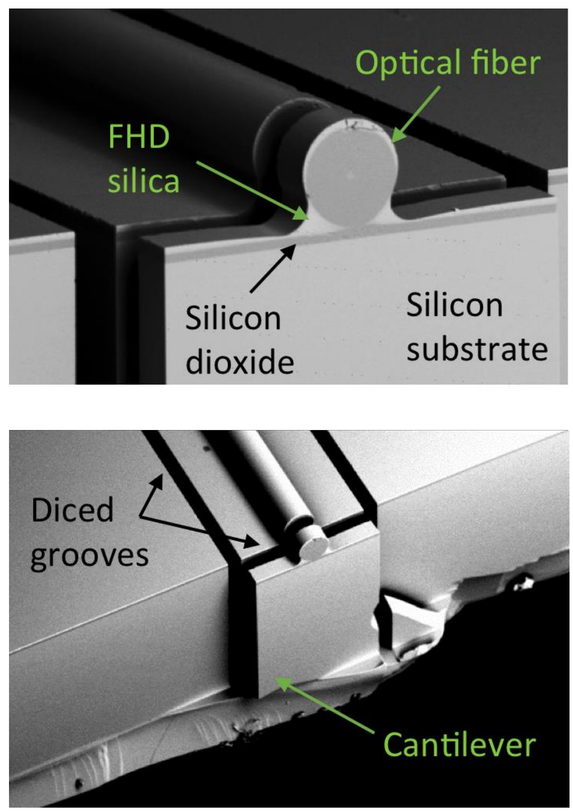

Fig. 1. Scanning electron microscope image of a physically micromachined integrated optical fiber-tip cantilever

It must be stressed that the fabrication approach reported solely uses physical micromachining and is therefore different to other reports that use a combination of physical machining and wet-etching [14].

II. Fabrication Technique

IOF adapts the commercial glass deposition technique FHD, which is commonly used for the fabrication of Array Waveguide Gratings (AWGs) and other silica based Planar Lightwave Circuits (PLCs). The adaptation made involves the pre-layering of an optical fiber to a planar substrate. In this instance a 1 mm thick silicon wafer with a 15 µm thick thermal oxide is used as the substrate. Following glass soot deposition, a consolidation is undertaken at high temperature (1250ºC), forming a miscible glass alloy between the optical fiber and thermal oxide. This results in a mechanically robust integrated platform that has the ability to optically guide both in the fiber and the FHD layer(s). It must be noted that in this demonstration the IOF is used solely for its mechanical properties, as all light is guided in the fiber.

Fabrication of the cantilever was achieved with the use of a precision dicing saw (Loadpoint Microace) and a nickel bonded synthetic diamond blade (DiscoTech ZH05-SD4800-NI-50-GG). The depth of cut chosen was 800 µm; rotation speed of 25 krpm and cutting speed of 0.1 mm/s. In total five cuts were made, two parallel and three orthogonal to the fiber. The orthogonal cuts formed air cavities of 59 µm (single cut) and 147 µm (dual cut) respectively and a glass cavity of 65 µm, as shown in Figure 2. To form a distal cantilever this structure was cleaved, which left only a single air and glass cavity.

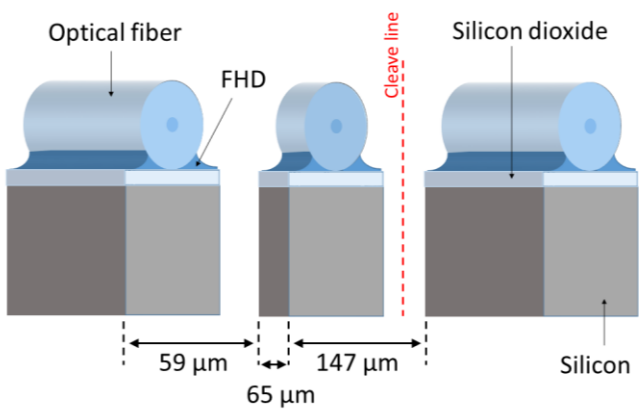

Fig. 2. Schematic side view of fabricated cantilever

The Sa surface roughness (which is an arithmetic mean height calculation) of the air-glass interfaces was measured to be 29 nm using a white light interferometer. This is larger than some previously reported results [15], which used a dicing blade containing much smaller grit (5000 grit size used not 4800). It must be noted that in order to achieve the depth-of-cut desired (800 µm) it was necessary to use the more course grit due to commercial availability at the time at which this script was written. Improved interface surface quality should be achievable without compromising sensitivity if further developments of commercial blades are made.

To understand the optical spectra resulting from these cavities a multi-cavity solution was formulated using signal flow graph analysis and Mason's rule.

III. Signal Flow Graphs and Mason's Rule

Optomechanical cantilevers with optical fiber readouts are nowadays routinely interrogated via reliable, low noise interferometers, which guarantee linear response over large displacements and accessing a frequency bandwidth of several tens of kHz without compromising the overall performance. The following approach uses spectrally broadband data and signal flow graph theory. It is not intended to be a method of optical measurement but rather a method of optical characterization and a route to infer spring constant of this and similar fiber-tip cantilever constructs, e.g. as part of design iteration and quality control assessment.

Signal flow graph analysis of layered media is considered to explain the spectral characteristics of the fabricated cavities. Using Mason's rule a graphical representation of a dynamic system of linear equations can be represented [16]. Figure 3 represents the pathway of light through a glass-air-glass-air interface. This technique can also be expanded to three cavities as in the pre-cleaved structure (shown in Figure 2) or indeed multiple cavities. With respect to nomenclature, t correspondence to transmission coefficient, r the reflection coefficient and θ is a phase term defined as:

$$\theta = \frac{2\pi\left(n_{eff}\, l\right)}{\lambda} \tag{1}$$

n_{eff} is the effective refractive index and l the propagation distance. Each node in the flow graph corresponds to the wave mode amplitude at an interface and the arrows define coupling terms from one node to another. The resultant closed loops being the cavity resonances. It is important to note that Masons rule yields the reflectance via inspection.

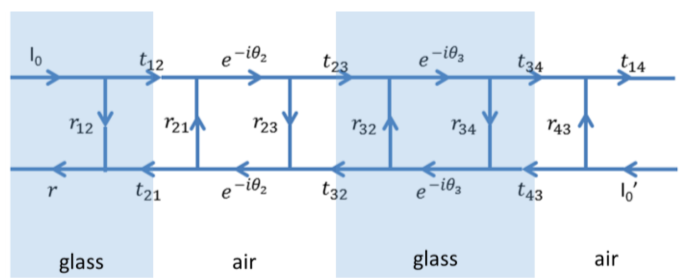

Fig. 3. Graphical representation of light transmitting and reflecting through a glass-air-glass-air cavity.

The amplitude transmitted through the structure can be obtained by summing all the different paths from source node to output node. Mason's Rule expresses this transfer function of the system as:

$$T = \frac{\sum_k P_k \Delta_k}{\Delta} \tag{2}$$

where the summation is made over all k-paths connecting the input to output node. Δ is the determinant of the system [16], P_k is the k^{th} forward path gain (product of gains found through traversing a succession of branches in the direction of arrows with no node passed more than once) and Δ_k is the determinant of the k^{th} forward loop.

IV. RESULTS

The back reflected spectra of the fabricated cavity was measured using a broadband SLED (Amonics, ASLD-CWDM-5-B-FA) and an Optical Spectrum Analyzer (OSA) (Ando AQ6317B). The observed spectra prior to cleaving (treble cavity) and after cleaving (double cavity) is illustrated in Figure 4. The spectral resolution of the OSA was set to 0.1 nm.

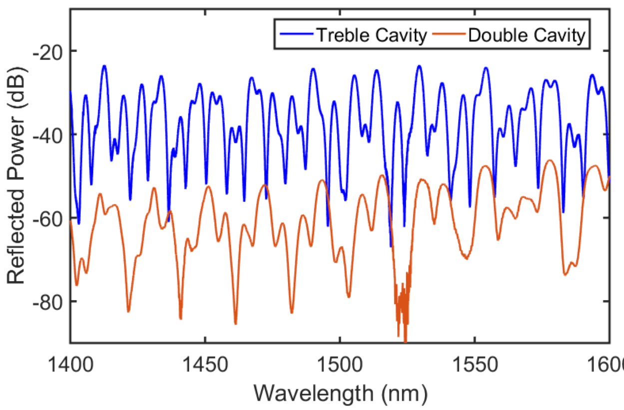

Fig. 4. Measured back reflection from the physically machined integrated fiber prior and post cleave

To highlight the periodic features from this optical spectra a Fourier transformation was made, shown in Figure 5, which compares the spectra before and after cleaving. This is compared to a theoretical frequency distribution calculated using Mason's rule, illustrated in Figure 6. It must be noted that the theoretical model also accounts for dispersion effects through use of accepted Sellmeier coefficients for silica, however the contribution of this term only marginally improved the fit.

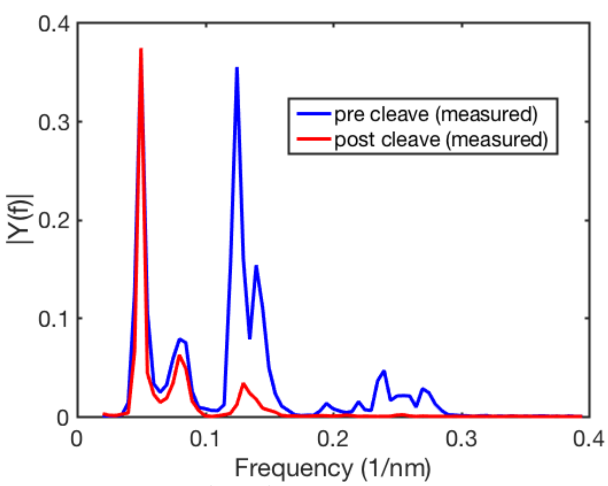

Fig. 5. The Fourier Transform of the measured spectral response pre and post cleave.

From Figure 5 and Figure 6 it is evident that the main resonance features appear comparable in both the measured and theoretical model. It is noted that variation in amplitude, |Y(f)|, between the theoretical and measured model is consistent with diffraction effects and recoupling in the air cavity sections. Additionally, there are also scattering losses at the interfaces between cavities. These parameters were not directly accounted for, but it is understood that divergence at an air gap of ~60 μm reduces fringe visibility by ~25 % [17].

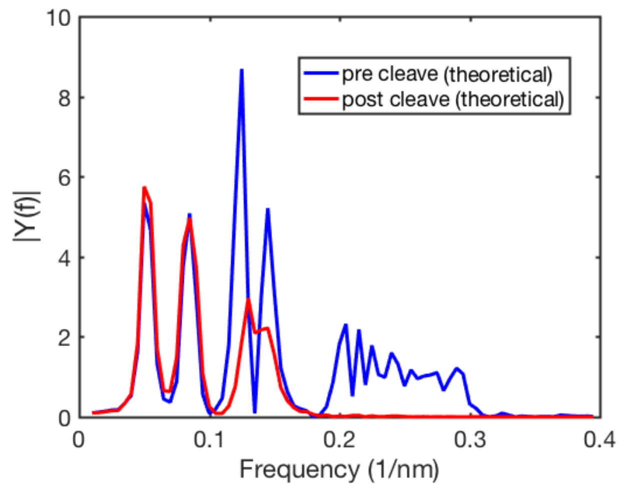

Fig. 6. The Fourier Transform of the theoretical spectral response pre and post cleave.

A. Force Calibration

Lateral force calibration was made using a KLA Tencor P16 stylus profiler. The forces applied are presented schematically in Figure 7. In the arrangement the stylus was translated such that its leading edge was the only point of contact with the chip. The stylus was scanned in the direction of forward light propagation and off to one side of the fiber, such that it did not touch the fiber.

The following treatment assumes that the cantilever was level and the stylus does not deflect or twist to a significant degree. The velocity of translation is assumed to be constant and therefore the system to have no net force.

The two forces acting on the stylus are the vertical load, F_{load}, and horizontal applied load, F_{tran}, that enabled a constant positive velocity, $\underline{v}$, along the x' component. For each applied load the velocity was kept at a constant 10 μm/s. To vary the force in the lateral component the preset values of vertical load were varied. The spectral data for this was taken and interpreted into cavity length changes using Masosn's rule.

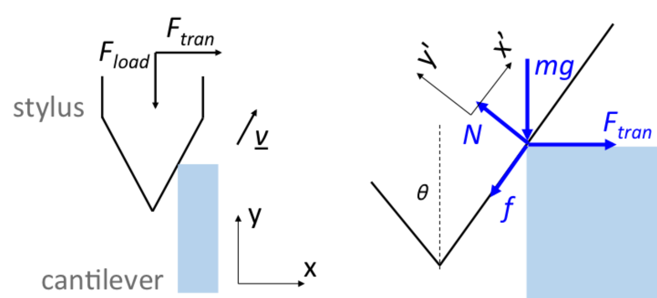

Fig. 7. Configuration of the stylus profiler and the components of applied force.

Variation in optical path lengths for the air and glass cavities were interpreted through fitting Mason's rule to the reflected spectra. In this case an ASE was used for interrogation (with a bandwidth ranging from 1530 nm to 1570 nm). The spectral response from these respective cavities with respect to applied load is shown in Figure 8. As expected, the air cavity has the greatest response to applied force, with a sensitivity of 0.17 ± 0.01 pm/nN. The error bars presented in Figure 8 are calculated from a 5 data point standard error for that load.

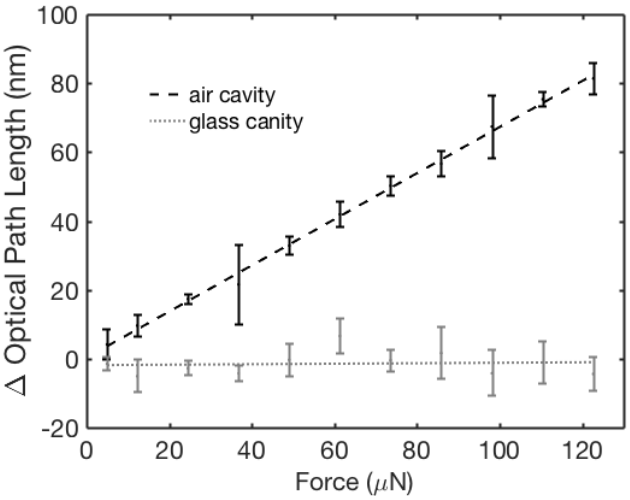

Fig. 8. Variation in optical path lengths of the air and glass cavities subject to mechanical actuation

A reduced chi-square calculation, χ^2, of 7.64 (2.d.p) was observed for the fiber cavity trend. This equates to a chi-square per degree of freedom (df=9) of 0.76 (2.d.p). Interpretation of this relates to a 57 % chance of obtaining a set of measurements at least this discrepant from the model, assuming the model to be true. As they form part of the same spectrum, it is not improbable that the measurements have an element of cross talk due to the nature of fitting.

An optical path length change (in the air cavity) and applied load can be interpreted in terms of the cantilever's end-tip displacement for a set lateral force. From these two values an estimation of spring constant can be made.

B. Estimating Spring Constant

The spring constant, k, for a cantilever is defined as the normal force, F_x, required for a unit normal displacement at the end-tip, Δ_x. The optical path length change in the air cavity, l_{air}, is approximately equal to the normal displacement of the cantilever's end-tip, for this considered geometry. The normal force along the x-component, N_x, can be derived as:

$$N_x = \frac{mg}{1 - \mu_k\sqrt{3}} \tag{3}$$

where μ_k is the constant for kinetic friction, approximated to be 0.115 [18] between silica (FHD layer) and diamond (profiler head), m is the set load mass and g is gravitational acceleration (9.81 ms^{-2}). Using the definition of spring constant, the gradient measured in Figure 8 and Equation 3 the following can derived:

$$k = \frac{F_x}{\Delta_x} \approx \frac{1}{1 - \mu_k\sqrt{3}}\left(\frac{d\Delta_{air}}{dF_{load}}\right)^{-1} \tag{4}$$

This gives an estimation of 740 ± 40 N/m for spring constant. Considering the simplified geometry of a purely silicon cantilever beam, without the optical fiber or FHD element. An analytical solution using the equation:

$$k = \frac{Ewt^3}{4L^3} \tag{5}$$

can be used, where Young's modulus, E, for silicon is taken to be 130 GPa; the width of the cantilever, w, 501 ± 1 μm; the thickness of the cantilever, t, 65 ± 1 μm and the cantilever length, L, 806 ± 5 μm. This calculated estimation gives a spring constant, k, equal to 850 ± 40 N/m.

This simplified approximation is an overestimation of the value inferred through measurement. It is noted however that the displacements measured at the fibre core are 62.5 μm (radius of fibre) above the position at which normal force is calculated, relating to an 8% underestimation of the measured value (horizontal difference trigonometrically equal to vertical difference 62.5/806 = 8%). This corresponds to a modified measured estimate of 790 ± 50 N/m, which overlaps the analytical approximation, with that inferred through profiler actuation.

C. Thermal Calibration

The thermal response of the cantilever is shown in Figure 9. The respective cavity responses were 2.3 nm/°C and 1.1 nm/°C for the air and glass cavities respectively.

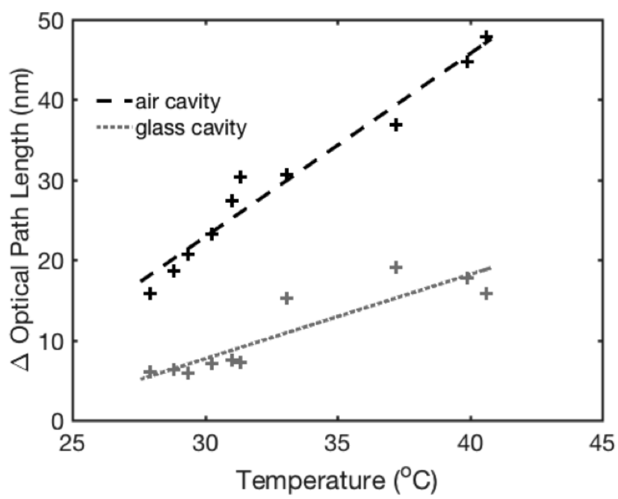

Fig. 9. Changes in optical path lengths of the air and glass cavities subject to thermal variation.

It is noted that the glass cavity has a significantly smaller thermal response than the air cavity. The reason for this is two-fold. Firstly the air cavity is dominated by the thermal expansion of the underlying silicon, which is approximately an order of magnitude greater than that of silica. Secondly the change in optical path length brought about through thermal expansion is opposed by silica's strain-optic coefficient.

V. Discussion

Mason's rule enables an approach for multi-cavity analysis. Most authors simulate FP cavities by either analyzing first- and second-order reflections [19], or through use of the S/T-matrix approach that inherently calculates the infinite amount of reflections occurring at the boundaries [20]. Mason's method arguably sits between these, enabling effective calculation of the visibility factor of the cavities. It needs to be stressed that the interrogation method presented here is intended only to be a tool for spectral and physical calibration. Dynamic mode methods shall be the consideration of future work.

The empirical estimation for spring constant was 790 ± 50 N/m, which was comparable to that expected for a cantilever of this dimension. This may be considered slightly stiff for some applications, such as those associated with AFM, where typically spring constants range between 300 N/m to 0.01 N/m. It should be noted that the spring constant of such a cantilever could feasibly be reduced further through fabrication if required. For example, considering Equation 5, thickness and length have a significant influence on the value. Using a combination of a thicker wafer and a blade capable of a deeper depth of cut, dimensions of up to 2 mm are feasible, which would give a $(2/0.8)^3 \approx 16$-fold reduction from the 0.8 mm depth of cut made in this demonstration. The thickness of the cantilever could also be reduced by half, giving a further 8-fold reduction. The width of the cantilever is 501 µm, through using a smaller diameter fiber and dicing it smaller this can be reduced to 60 µm width, giving a reduction of approximately 8-fold. Furthermore silica could be used instead of silicon, which has a Young's modulus of 73 GPa and so would approximately half the spring constant. In combination spring constants below 1 N/m are entirely feasible, which is approaching the highest performance end of commercial AFMs.

It was shown that through using two distinct optical cavities a degree of thermal compensation can be made. However, in this particular configuration thermal compensation does not have the precision of alternative approaches such as Fiber Bragg gratings (FBGs) [12], [13]. Future work will therefore consider architectures that enhance this thermal response or use the technique in combination with FBGs. The solution dictated largely by the application e.g. at elevated temperatures the use of FBGs may not be possible.

VI. Conclusions

The first demonstration of a fiber-tip cantilever in an Integrated Optical Fiber (IOF) platform has been shown. IOF is proven to be a robust method capable of withstanding the mechanical rigors of physical micromachining. The microstructured cantilever is optically monitored and thus has immunity to electromagnetic interference and considered safe in flammable environments. This is the first reported demonstration that uses only physical micromachining to achieve microstructures, all other approaches reported have been in combination with other cleanroom toolsets such as wet etching.

The use of Mason's rule to interpret multicavity spectra using was demonstrated. Through the interpretation deflection monitoring of the cantilever can be made. This is a useful tool to infer spectral shifts and to estimate the spring constant if the cantilever simultaneously undergoes known force actuation. A spring constant of 790 ± 50 N/m was empirically estimated using this technique. Through further development of design parameters the stiffness could be reduced further making it comparable to AFM gold standards.

It was demonstrated that thermal variation could be inferred through monitoring spectral features associated with the glass cavity. However, this may only be of significance over other techniques at elevated temperatures.

References

[1] S. Poeggel, D. Tosi, G. Leen, and E. Lewis, "Miniature low-cost extrinsic Fabry-Perot interferometer for low-pressure detection," *Proc. SPIE* 8788, Optical Measurement Systems for Industrial Inspection VIII, 878811, May 13, 2013.

[2] Y. J. Rao, "Recent progress in fiber-optic extrinsic Fabry-Perot interferometric sensors," *Opt. Fiber Technol.*, vol. 12, no. 3, pp. 227–237, 2006.

[3] C. J. Misas, F. M. M. Araújo, L. A. Ferreira, J. L. Santos, and J. M. López-Higuera, "Interrogation of low-finesse Fabry-Pérot cavities based on modulation of the transfer function of a wavelength division multiplexer," *J. Light. Technol.*, vol. 19, no. 5, pp. 673–681, 2001.

[4] A. Cipullo, G. Gruca, K. Heeck, F. De Filippis, D. Iannuzzi, A. Minardo, and L. Zeni, "Numerical study of a ferrule-top cantilever optical fiber sensor for wind-tunnel applications and comparison with experimental results," *Sensors Actuators, A Phys.*, vol. 178, pp. 17–25, 2012.

[5] S. V. Beekmans and D. Iannuzzi, "Characterizing tissue stiffness at the tip of a rigid needle using an opto-mechanical force sensor," *Biomed. Microdevices*, vol. 18, no. 1, pp. 15, 2016.

[6] H. van Hoorn, N. A. Kurniawan, G. H. Koenderink, and D. Iannuzzi, "Local dynamic mechanical analysis for heterogeneous soft matter using ferrule-top indentation," *Soft Matter*, vol. 12, pp. 3066–3073, 2016.

[7] B. Tiribilli, G. Margheri, P. Baschieri, C. Menozzi, D. Chavan, and D. Iannuzzi, "Fibre-top atomic force microscope probe with optical near-field detection capabilities," *J. Microsc.*, vol. 242, no. 1, pp. 10–14, 2011.

[8] D. Iannuzzi, M. Slaman, J. H. Rector, H. Schreuders, S. Deladi, and M. C. Elwenspoek, "A fiber-top cantilever for hydrogen detection," *Sensors Actuators, B Chem.*, vol. 121, no. 2, pp. 706–708, 2007.

[9] D. Iannuzzi, S. Deladi, V. J. Gadgil, R. G. P. Sanders, H. Schreuders, and M. C. Elwenspoek, "Monolithic fiber-top sensor for critical environments and standard applications," *Appl. Phys. Lett.*, vol. 88, no. 5, pp. 1–3, 2006.

[10] K. B. Gavan, J. H. Rector, K. Heeck, D. Chavan, G. Gruca, T. H. Oosterkamp, and D. Iannuzzi, "Top-down approach to fiber-top cantilevers.," *Opt. Lett.*, vol. 36, no. 15, pp. 2898–2900, 2011.

[11] L. G. Carpenter, C. Holmes, H. L. Rogers, P. G. R. Smith, and J. C. Gates, "Integrated optic glass microcantilevers with Bragg grating interrogation.," *Opt. Express*, vol. 18, no. 22, pp. 23296–301, Oct. 2010.

[12] C. Holmes, J. C. Gates, and P. G. R. Smith, "Planarised optical fiber composite using flame hydrolysis deposition demonstrating an integrated FBG anemometer," *Opt. Express*, vol. 22, no. 26, pp. 32150, Dec. 2014.

[13] S. G. Lynch, C. Holmes, S. A. Berry, C. James, A. Jantzen, T. I. Ferreiro, and P. G. R. Smith, "External cavity diode laser based upon an FBG in an integrated optical fiber platform," vol. 24, no. 8, pp. 22781–22788, 2016.

[14] C. Holmes, L. G. Carpenter, H. L. Rogers, J. C. Gates, and P. G. R. Smith, "Quantifying the optical sensitivity of planar Bragg gratings in glass micro-cantilevers to physical deflection," *J. Micromechanics Microengineering*, vol. 21, no. 3, pp. 35014, 2011.

[15] L. G. Carpenter, H. L. Rogers, P. A. Cooper, C. Holmes, J. C. Gates, and P. G. R. Smith, "Low optical-loss facet preparation for silica-on-silicon photonics using the ductile dicing regime," *J. Phys. D. Appl. Phys.*, vol. 46, pp. 475103, 2013.

[16] S. J. Mason, "Feedback theory: further properties of signal flow graphs," in *Proceedings of the I.R.E*, 1955, vol. 44, no. 7, pp. 920–926.

[17] V. Arya, M. de Vries, K. A. Murphy, A. Wang, and R. O. Claus, "Exact Analysis of the Extrinsic Fabry-Perot Interferometric Optical Fiber Sensor Using Kirchhoff's Diffraction Formalism," *Opt. Fiber Technol.*, vol. 1, pp. 380–384, 1995.

[18] A. Yurkov, V. Skvortsov, I. Buyanovsky, and R. Matvievsky, "Sliding friction of diamond on steel, sapphire, alumina and fused silica with and without lubricants," *J. Mater. Sci. Lett.*, vol. 16, no. 16, pp. 1370–1374, 1997.

[19] K. Bremer, E. Lewis, G. Leen, B. Moss, S. Lochmann, and I. Mueller, "Feedback Stabilized Interrogation Technique for EFPI / FBG hybrid Fibre Optic Pressure and Temperature Sensors," *IEEE Sens. J.*, vol. 12, no. 1, pp. 133-138, 2011.

[20] D. Tosi, "Simultaneous Detection of Multiple Fiber-Optic Fabry-Perot Interferometry Sensors with Cepstrum-Division Multiplexing," *J. Light. Technol.*, vol. 34, no. 15, pp. 3622–3627, 2016.

Christopher Holmes is currently a Senior Enterprise Fellow at the Optoelectronics Research Centre, University of Southampton. He received a First Class Masters degree in Physics from the University of Warwick (2004) and after a period in industry, returned to academia to complete a PhD at the University of Southampton (2010). His thesis was on silica integrated optics and CASE supported by the photonics company Stratophase Ltd. He continues to engage with industry and is a theme leader for the University of Southampton multidisciplinary initiative MENSUS (Monitoring of Engineered and Natural Systems Using Sensors).

Alexander Jantzen is currently a PhD student at the Optoelectronics Research Centre after having received a first class masters of physics from the University of Southampton in 2015. His research interests are focused on designing, fabricating and developing integrated micro opto-mechanical system components for sensing in harsh environments with a focus on silica devices aimed at aerospace use.

Alan C. Gray graduated with a BSc in Experimental Physics in 2014 from Maynooth University and an MSc in Applied Physics in 2015 from the University of Limerick. Alan is currently a postgraduate researcher in the Optical engineering and Quantum Photonics group at the Optoelectronics Research Centre. His research interests are in integrated photonic structures for quantum applications.

Lewis G. Carpenter is a Knowledge Transfer Partnership (KTP) associate working with Covesion Ltd. and the Optoelectronics Research Centre (ORC). He received a first class Bachelors in Electrical Engineering from the University of Southampton (2009) and won the National Grid award for the highest awarded dissertation mark. Lewis continued his studies at Southampton within the ORC, under the supervision of Prof. Smith and Dr. Gates and was awarded his Ph.D in 2013. His PhD focused on precision dicing (sawing) and micromilling techniques for silica photonic device fabrication and particularly for the production of micro optomechanical sensors and ultra-smooth micron scale features for integrated optics. Working as a Research Fellow (2014) Lewis researched the integration of precision micromilled structures with photonic waveguides for the application to optofluidic evanescent field sensing. Currently as a KTP associate he develops ridge waveguides in PPLN (Periodically Poled Lithium Niobate) for high efficient wavelength conversion, with special interested in the application of these technologies to atom/ion trapping and single photon sources.

Paul C. Gow received his PhD in Physics in 2016 from the University of Southampton. He is currently working in the Optical engineering and Quantum Photonics group at the Optoelectronics Research Centre. His main research interests are in enabling Quantum Technologies, Direct UV written planar photonics devices and laser machining of silica photonic structures.

Stephen G. Lynch is currently a research fellow in the Optoelectronics Research Centre (ORC). He received a BEng degree from the University of Southampton in 2012 in Electronic Engineering. Currently, for his research Stephen is investigating planar Bragg-grating stabilized lasers and locking them to stable external resonators using novel feedback control techniques.

James C. Gates is currently a Principle Research Fellow in the ORC. He received a M.Phys degree from the University of Southampton in 1999, he continued his studies at Southampton in the Optoelectronics Research Centre (ORC) and in 2003 received a Ph.D in optoelectronics. His Ph.D. thesis investigated the optical properties of various photonic devices at a nanometer scale using an interferometric near-field technique. After his PhD moved back to the department of physics in Southampton and worked in the field of nanophotonics, before returning to the ORC in 2006. He currently develops fabrication techniques for manufacturing photonic devices, principally planar-integrated optical devices. He has worked on applications in sensing, telecommunications and quantum optics.

Peter G.R. Smith is a Professor in the Optoelectronics Research Centre and in Electronics and Computer Science at the University of Southampton. He graduated from Oxford University with a BA in Physics in 1990 and D.Phil in Nonlinear Optics in 1993. After a year spent as a management consultant he joined the University of Southampton. Peter has worked on a number of areas in optics research ranging from laser spectroscopy to polymer integrated-optics. He has published over 180 journal and conference papers in the fields of periodically poled materials and UV written devices at major conferences, including invited talks at national and international meetings.